[7]The general method of producing F_A centers is described by H. Hartel and F. Lüty, Z. Physik 177, 369 (1964). The present temperatures and wavelengths are selected to maximize the production rates in the present crystal systems.

[8]D. Frölich and H. Mahr, Phys. Rev. 148, 868 (1966).

[9]Figure 6(b) of Ref. 4.

[10]G. Spinolo and F. C. Brown, Phys. Rev. 135, A450 (1964).

[11]Reference 3, pp. 228–236.

PHYSICAL REVIEW B VOLUME 1, NUMBER 12 15 JUNE 1970

Theory of Light Scattering from Polaritons in the Presence of Lattice Damping

H. J. Benson and D. L. Mills†
Department of Physics, University of California, Irvine, Irvine, California 92664
(Received 9 February 1970)

We formulate the theory of light scattering from polaritons in ionic crystals by a Green's-function method. The theory is presented in a form that allows the effect of the damping of the lattice motion to be included in a rigorous fashion. Difficulties encountered in earlier phenomenological approaches to the problem are eliminated by the present work. It is pointed out that, in principle, detailed studies of the shape of the Raman line may be utilized to determine the frequency dependence of the phonon proper self-energy over a wide range of frequencies. We present the results of numerical studies of the shape and position of the Raman line as a function of scattering angle, for the case where the frequency dependence of the proper self-energy is ignored. We find that even when the damping of the lattice is appreciable, the position of the line center as a function of scattering angle is given accurately by employing the polariton dispersion relation appropriate to the case where *no* damping is present.

I. INTRODUCTION

The transverse optic (TO) phonons of long wavelength generate a macroscopic electromagnetic (EM) wave when they are excited. As a consequence, the long-wavelength normal modes of an ionic crystal are mixed modes, involving both lattice motion and the EM field. These mixed modes are called "polaritons." The study of the Raman scattering of light from these modes has provided useful information about the properties of polaritons, and a number of other properties of ionic crystals.[1] Since the polariton modes contain roughly an equal admixture of lattice motion and EM field when the wave number q of the polariton is near ω_{TO}/c, where ω_{TO} and c are the frequency of the TO phonon and the velocity of light, experimental study of these modes requires observation of the Raman effect in the near forward direction. This is because ω_{TO}/c is small compared to the wave vector of light employed in these experiments.

The theory of the Raman scattering from polaritons was first discussed by Loudon.[2] In many discussions of the experimental data, one ignores the effect of the damping of the lattice motion on the spectrum of the scattered light. One then obtains a line that has zero width, i.e., the radiation leaving the crystal contains spectral components at $\pm\omega_\pi(\vec{q})$, where $\omega_\pi(\vec{q})$ is the polariton frequency appropriate to the particular scattering angle examined. In real crystals, the lattice motion is damped, either by anharmonic effects or by crystal imperfections. The finite lifetime of the TO phonon will cause the spectral distribution to scattered light to be spread out in frequency, and will also shift the position of the center of the Raman line. The purpose of this paper is to present a theory of the line shape and frequency shift, and to discuss the kind of information one may obtain by studying these quantities.

A phenomenological means of describing the position of the line center has appeared in a number of papers.[3] In the absence of any damping, the polariton dispersion relation may be written in the form

$$c^2q^2/\omega^2 = \epsilon(\omega) = \epsilon_0 + 4\pi\beta\omega_{TO}^2/(\omega_{TO}^2 - \omega^2) \ , \qquad (1)$$

where ϵ_0 is the high-frequency (optical) dielectric constant, and β is the contribution of the lattice to the static polarizability of the crystal. Polariton dispersion curves computed for parameters appropriate to ZnSe are given in Fig. 1. One then includes the effect of the damping on the dispersion relation by replacing the right-hand side of Eq. (1) by $\epsilon_R(\omega)$, the real part of the dielectric

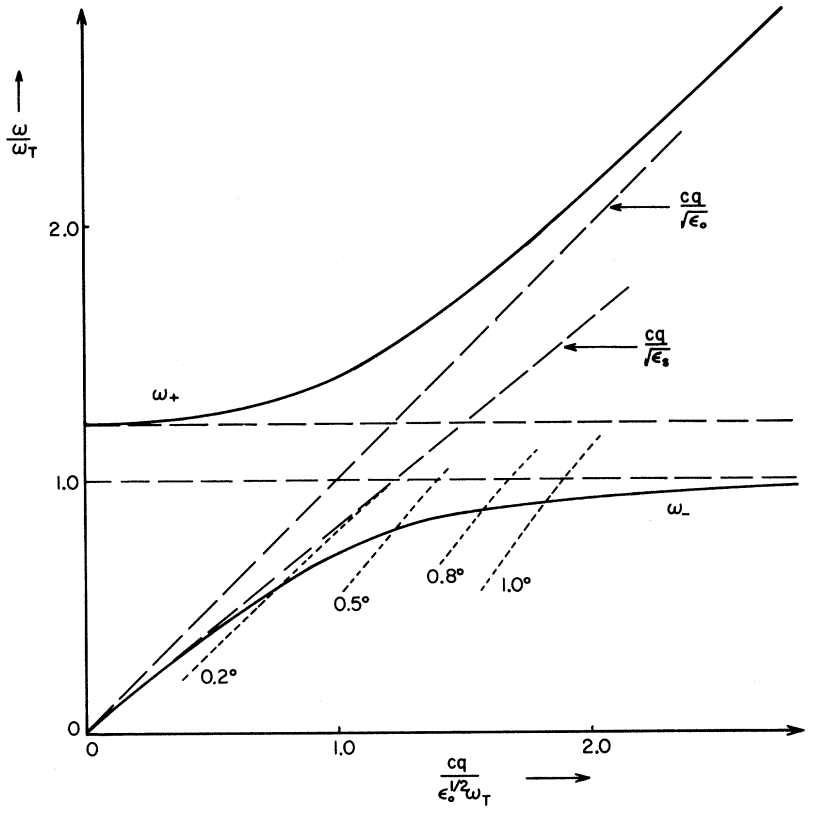

FIG. 1. Polariton dispersion curves for ZnSe, ignoring the effect of damping of the lattice motion. The quantities ϵ_s and ϵ_0 are the static and high-frequency dielectric constants, respectively. The dashed curves give the relation between frequency transfer and wave-vector transfer for various scattering angles.

constant $\epsilon(\omega)$. In Fig. 2, we give the form in the presence of damping obtained by the procedure just described. The dispersion curves in Fig. 2 are then regarded as the dispersion curve for the excitations of the medium.

There are three serious shortcomings of the procedure described in the preceding paragraph. First of all, the lower hair-pin-shaped branch turns back when the wave number q is equal to the value q_c indicated in the figure. It is quite clear that one cannot obtain a description of large-angle Raman scattering from TO phonons using this description. One has to use different theories to describe large-angle Raman scattering and small-angle scattering in the polariton regime. The existence of this turnaround at q_c has caused Puthoff *et al.*[3] to suggest that the nature of the normal modes should change qualitatively as q passes through q_c, although these authors found the scattering intensity to vary smoothly with angle in this regime. Another difficulty is that when the damping is large, q_c becomes quite small, and the dispersion curve of Fig. 2 turns about at very small scattering angles. Third, for $q < q_c$, Fig. 2 indicates the presence of three distinct portions of the dispersion curve. This suggests that one might see some evidence of the middle piece in the scattering spectra, although no such effect has been reported so far.

The difficulty with the use of Fig. 2 stems from an improper description of the nature of the excitation in the medium in the presence of damping. One attempts to describe the excitation in the medium by a "sharp" well-defined wave vector $\vec{q}$ and a well-defined frequency ω. This kind of description is inappropriate in the presence of damping, where the excitation has a finite lifetime and a finite mean free path.

The Green's-function method allows one to study the spectrum of radiation scattered inelastically from crystals, without the need of assigning a well-defined frequency and wave vector to the excitation in the medium. In the Green's-function formulation, the variables that enter the theory in a natural fashion are the frequency shift $\omega = \omega_1 - \omega_S$ and wave-vector transfer $\vec{q} = \vec{k}_I - \vec{k}_S$ suffered by the exciting radiation. If the crystal is transparent, these quantities are real, and are given once the scattering geometry is known.

In this paper, we present the theory of light scattering from polaritons, for the case when anharmonic damping of the lattice motion is important. By employing a Green's-function method, we obtain an expression for the scattering cross sec-

tion that applies in the polariton regime and to the large-angle regime. We also present numerical studies of the line shape and linewidth as a function of scattering angle in the polariton regime. In general, the intrinsic width of the line is found to vary with scattering angle, and the line is also asymmetric. The source of the asymmetry is the variation with frequency of the admixture of the electro-optic and atomic displacement contributions to the cross section, at fixed scattering angle. A quantitative study of these effects and a discussion of their dependence on the properties of the crystal are presented below.

We also find that the position of the polariton line as a function of scattering angle is accurately given if the data are interpreted by assuming that the position of the peak is given by the polariton dispersion relation, in the absence of damping. This is so even when an appreciable amount of damping is present.

It is pointed out that a detailed study of the polariton line shape as a function of scattering angle provides a means of determining the frequency dependence of the proper self-energy $\Pi(q, \Omega)$ of the TO phonon, at $\vec{q} \simeq 0$. Infrared and large-angle Raman studies of the intrinsic width of the TO mode generally provide information about only $\mathrm{Im}[\Pi(0, \omega_{TO})]$.[4]

II. DERIVATION OF RAMAN CROSS SECTION

The interaction between the external electric field $\vec{E}(\vec{r}, t)$ and the excitations of the medium will be described by adding to the Hamiltonian H_0 of the crystal the term

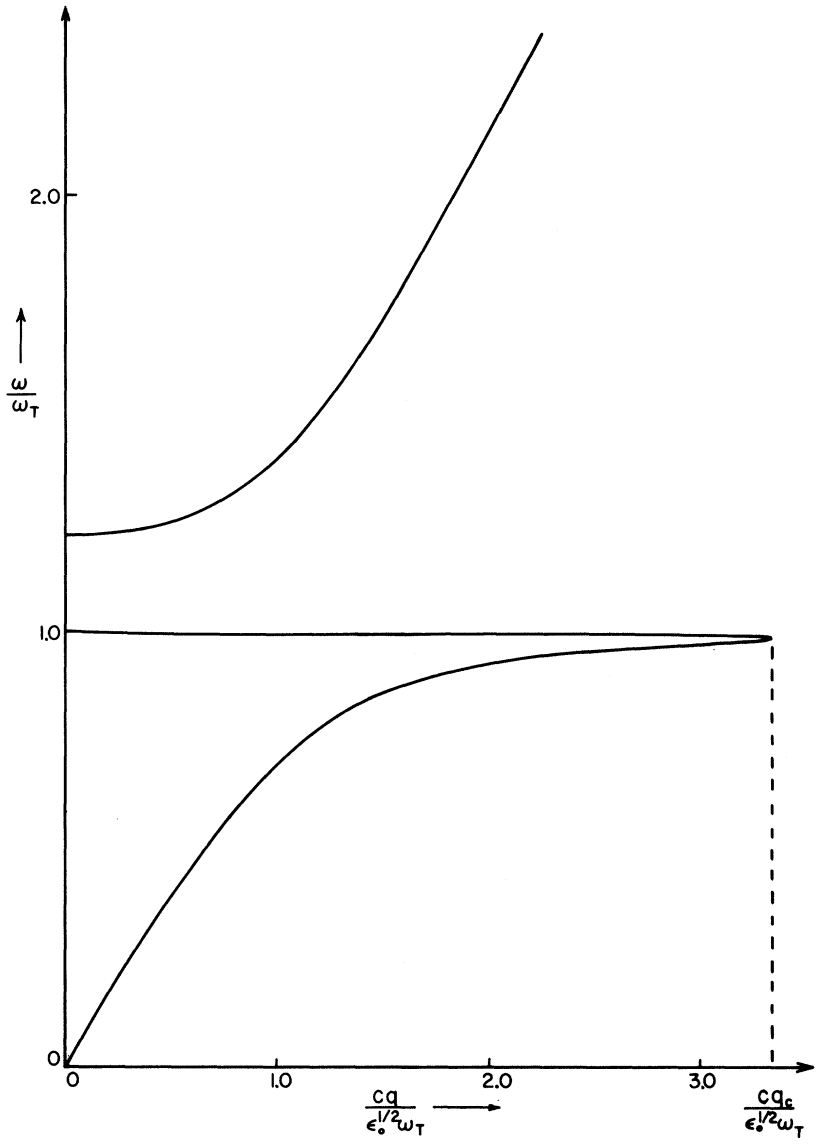

FIG. 2. Dispersion curves computed for parameters relevant to ZnSe, from the relation $c^2q^2 = \omega^2\epsilon_R$, where ϵ_R is the real part of the dielectric constant in the presence of damping. The curves shown have been computed for the damping constant $\Gamma = 2.5\ \mathrm{cm}^{-1}$. The turnaround wave vector q_c decreases with increasing Γ.

$$H_1 = -\tfrac{1}{2}\int d\vec{r}\,\Delta\vec{P}^{\,e}(\vec{r})\cdot\vec{E}(\vec{r}) \quad , \tag{2}$$

where the operator $\Delta\vec{P}^{\,(e)}(\vec{r})$ is the change in the electronic contribution to the electric dipole moment of the crystal produced by an excitation of the medium. There are two contributions to $\Delta\vec{P}^{\,(e)}(\vec{r})$ when a polariton is excited. The first is the atomic displacement contribution that has its origin in the dependence of the dielectric polarizability χ on the relative positions of the ions, and the second is associated with the dependence of χ on the electric field. Excitation of a polariton generates a macroscopic field $\vec{\mathcal{E}}^{\,\pi}$ in the crystal, and in noncentrosymmetric crystals a change in χ of first order in $\mathcal{E}_\pi$ occurs.

Let us consider an optical mode in a crystal with two atoms per unit cell. We consider long-wavelength modes, and take the operator $\vec{u}$ to represent the relative displacement between ions in the unit cell. We make a continuum model, and treat $\vec{u}(\vec{x}, t)$ as a continuous function of position. Then assuming $\Delta\vec{P}^{\,e}(\vec{r})$ depends only on the local values of the electric fields and displacement $\vec{u}$, we have

$$\Delta P^e_\alpha(\vec{r}) = \sum_{\beta\gamma}\{a_{\alpha\beta;\gamma}u_\gamma(\vec{r}) + b_{\alpha\beta;\gamma}\,\mathcal{E}^\pi_\gamma(\vec{r})\}E_\beta(\vec{r}) \quad . \tag{3}$$

The quantity $a_{\alpha\beta;\gamma}$ is the atomic displacement susceptibility tensor, and $b_{\alpha\beta;\gamma}$ is the electro-optic tensor. For crystals of the zinc-blende structure, the third-rank tensors $a_{\alpha\beta;\gamma}$ and $b_{\alpha\beta;\gamma}$ have only one independent component:

$$a_{\alpha\beta;\gamma} = a\,|\epsilon_{\alpha\beta\gamma}|, \quad b_{\alpha\beta;\gamma} = b\,|\epsilon_{\alpha\beta\gamma}| \quad ,$$

where $\epsilon_{\alpha\beta\gamma}$ is the Levi-Civita symbol. Thus,

$$H_1 = -\sum_{\alpha\beta\gamma}\int \tfrac{1}{2}dr\{a_{\alpha\beta;\gamma}u_\gamma + b_{\alpha\beta;\gamma}\,\mathcal{E}^\pi_\gamma\}E_\beta E_\alpha \, . \tag{4a}$$

We now write the electric field operator $\vec{E}(\vec{r})$ and the vector potential $\vec{A}(\vec{r})$ in the form

$$E_\alpha(\vec{r}) = \left(\frac{4\pi}{\epsilon_0 V}\right)^{1/2}\sum_{\vec{k}\lambda}\hat{e}_\alpha(\vec{k}\lambda)\Pi_{\vec{k}\lambda}e^{i\vec{k}\cdot\vec{r}} \tag{4b}$$

and $$A_\alpha(\vec{r}) = \left(\frac{4\pi c^2}{\epsilon_0 V}\right)^{1/2}\sum_{\vec{k}\lambda}\hat{e}_\alpha(\vec{k}\lambda)A_{\vec{k}\lambda}e^{i\vec{k}\cdot\vec{r}} \quad , \tag{4c}$$

where ϵ_0 is the high-frequency dielectric constant, V is the crystal volume, $\hat{e}(\vec{k}\lambda)$ is the polarization vector of the mode $(\vec{k}\lambda)$, and

$$A_{\vec{k}\lambda} = \left(\frac{\hbar}{2\omega_{\vec{k}}}\right)^{1/2}(a_{\vec{k}\lambda} + a^\dagger_{-\vec{k}\lambda}) \quad , \tag{4d}$$

$$\Pi_{\vec{k}\lambda} = i(\tfrac{1}{2}\hbar\omega_{\vec{k}})^{1/2}(a_{\vec{k}\lambda} - a^\dagger_{-\vec{k}\lambda}), \tag{4e}$$

with $\omega_{\vec{k}} = ck/\sqrt{\epsilon_0}$. The $a_{\vec{k}\lambda}$ and $a^\dagger_{\vec{k}\lambda}$ are the usual boson annihilation and creation operators that satisfy the commutation relations

$$[a_{\vec{k}\lambda},\ a^\dagger_{\vec{k}'\lambda'}] = \delta_{\vec{k}\vec{k}'}\,\delta_{\lambda\lambda'} \quad .$$

It follows that

$$[A_{\vec{k}\lambda},\ \Pi^\dagger_{\vec{k}'\lambda'}] = i\hbar\delta_{\vec{k}\vec{k}'}\delta_{\lambda\lambda'} \quad .$$

Also note $A_{\vec{k}\lambda} = A^\dagger_{-\vec{k}\lambda}$ and $\Pi_{\vec{k}\lambda} = \Pi^\dagger_{-\vec{k}\lambda}$.

Inserting the expansion of Eq. (4) into Eq. (3), and retaining only terms that describe Raman scattering of the incident photon gives

$$H_1 = \frac{2\pi\hbar}{\epsilon_0 V}\sum_{\alpha\beta\gamma}\sum_{\vec{k}\lambda,\,\vec{k}'\lambda'}(\omega_{\vec{k}}\omega_{\vec{k}'})^{1/2}\hat{e}_\alpha(\vec{k}\lambda)\hat{e}_\beta(\vec{k}'\lambda')a^\dagger_{\vec{k}'\lambda'}a_{\vec{k}\lambda}$$
$$\times\int d\vec{r}\,e^{i\vec{q}\cdot\vec{r}}(a_{\alpha\beta;\gamma}u_\gamma + b_{\alpha\beta;\gamma}\,\mathcal{E}^\pi_\gamma) \quad , \tag{5}$$

where $\vec{q} = \vec{k} - \vec{k}'$ is the wave-vector transfer suffered by the photon. We may now compute the Raman efficiency employing the form in Eq. (5), and the Fermi golden rule. The calculation proceeds precisely along the lines of Van Hove's classical discussion of the scattering of crystals.[5] It is convenient to write $\vec{u}(\vec{r})$ in the form

$$\vec{u}(\vec{r}) = \frac{1}{(Nm)^{1/2}}\sum_{\vec{q}}\hat{\epsilon}^{\,(\mathrm{ph})}(\vec{q})\,Q_{\vec{q}}\,e^{i\vec{q}\cdot\vec{r}} \quad .$$

In this expression, N is the number of unit cells in the crystal, m is reduced mass of the unit cell, $\hat{\epsilon}^{\,(\mathrm{ph})}(\vec{q})$ is the polarization vector associated with the phonon, and $Q_{\vec{q}}$ is the normal coordinate of the mode. We consider the scattering produced by a single phonon branch, so no branch index appears. We also use a Fourier decomposition of the polariton electric field $\vec{\mathcal{E}}^{\,\pi}(\vec{r})$ the same as that given in Eq. (4b).

For crystals of the zinc-blende structure where $a_{\alpha\beta;\gamma}$ and $b_{\alpha\beta;\gamma}$ have the form given above, we find the differential Raman efficiency per unit length, per unit solid angle, per unit frequency range $d^2S/d\Omega\,d\omega$ is given by

$$\frac{d^2S}{d\Omega\,d\omega} = \frac{\hbar V_c\omega_I^4}{mc^4}\left|\sum_{\alpha\beta\gamma}\hat{e}_\alpha(I)\hat{e}_\beta(S)\hat{\epsilon}^{\,(\mathrm{ph})}_\gamma|\epsilon_{\alpha\beta\gamma}|\right|^2$$
$$\times\int_{-\infty}^{+\infty}\frac{dt}{2\pi}\,e^{i\omega t}\Big[\,a^2\langle Q_{\vec{q}}(0)Q^\dagger_{\vec{q}}(t)\rangle$$
$$+\left(\frac{4\pi m}{\epsilon_0 V_c}\right)^{1/2}ab\,\langle\Pi_{\vec{q}}(0)Q^\dagger_{\vec{q}}(t)\rangle$$
$$+\left(\frac{4\pi m}{\epsilon_0 V_c}\right)^{1/2}ab\,\langle Q_{\vec{q}}(0)\Pi^\dagger_{\vec{q}}(t)\rangle$$
$$+\frac{4\pi m}{\epsilon_0 V_c}\,b^2\langle\Pi_{\vec{q}}(0)\Pi^\dagger_{\vec{q}}(t)\rangle\Big] \quad . \tag{6}$$

In Eq. (6), ω_I is the incident frequency, V_c is the

volume of the unit cell, $\omega = \omega_I - \omega_S$ is the frequency shift experienced by the light, and the vectors $\hat{e}(I)$ and $\hat{e}(S)$ are the polarization vectors of the incident and scattered light, respectively. The angular brackets denote an average over the appropriate statistical ensemble.

The correlation functions in Eq. (6) may be computed from standard prescriptions of many-body theory. If we have two operators A and B, we define the retarded Green's function

$$G_{AB}^{(R)}(t) = -i\theta(t)\langle[A(t), B(0)]\rangle \equiv \langle\langle(A(t),\ B(0))\rangle\rangle_R ,$$

where $\theta(t) = 1, \quad t > 0$

$= 0, \quad t < 0$.

Then we define the spectral density $\mathcal{A}_{AB}(\omega)$ by the relation

$$\mathcal{A}_{AB}(\omega) = (1/i)\left[G_{AB}^{(R)}(\omega - i\epsilon) - G_{AB}^{(R)}(\omega + i\epsilon)\right] ,$$

with $G_{AB}^{(R)}(\omega) = \int \frac{dt}{2\pi}\, e^{i\omega t} G_{AB}^{(R)}(t)$.

Correlation functions of the type encountered in Eq. (6) are then directly related to $\mathcal{A}_{AB}(\omega)$:

$$\int_{-\infty}^{+\infty} \frac{dt}{2\pi}\, e^{i\omega t}\langle A(0)B(t)\rangle = \{1 + n(\omega)\}\,\mathcal{A}_{AB}(\omega) ,$$

where $n(\omega) = (e^{\hbar\omega/k_BT} - 1)^{-1}$.

Equation (6) may then be written in the form

$$\frac{d^2S}{d\Omega\, d\omega} = \frac{\hbar V_c \omega_I^4}{mc^4}\left|\sum_{\alpha\beta\gamma} \hat{e}_\alpha(I)\hat{e}_\beta(S)\hat{\epsilon}_\gamma^{(\mathrm{ph})}\,|\epsilon_{\alpha\beta\gamma}|\right|^2 [1 + n(\omega)]$$
$$\times\Bigg[\, a^2\,\mathcal{A}_{QQ}(\vec{q}, \omega) + ab\left(\frac{4\pi m}{\epsilon_0 V_c}\right)^{1/2}\mathcal{A}_{\pi Q}(\vec{q}, \omega)$$
$$+ ab\left(\frac{4\pi m}{\epsilon_0 V_c}\right)^{1/2}\mathcal{A}_{Q\pi}(\vec{q}, \omega) + \frac{4\pi m}{\epsilon_0 V_c}\, b^2\,\mathcal{A}_{\pi\pi}(\vec{q}, \omega)\Bigg] . \quad (7)$$

This last result provides a general expression for the Raman cross section, once the correlation functions in Eq. (7) are known. We shall turn our attention to the computation of these functions in Sec. III. Note that the wave vector $\vec{q}$ and frequency ω are the wave-vector transfer and frequency shift of the incident photon; both of these quantities are real and are well defined in any particular experimental measurement.

III. FORM OF GREEN'S FUNCTIONS

In this section, we find the form of the various Green's functions and associated spectral densities that appear in Eq. (7). In order to do this, we now need to consider a detailed model of the lattice motion and the electric fields generated by the lattice motion.

We let $Q_{\vec{q}}$ be the normal coordinate associated with a long-wavelength TO phonon, in the absence of coupling between the lattice and the EM field. The symbol $P_{\vec{q}}$ will denote the momentum cannonically conjugate to $Q_{\vec{q}}$. The Hamiltonian will be taken to be a sum of four terms:

$$H = H_{\mathrm{ph}} + H_{\mathrm{EM}} + H_{\mathrm{EM\text{-}ph}} + H_A(\{Q_{\vec{q}}\}) , \quad (8)$$

where $H_{\mathrm{ph}} = \frac{1}{2}\sum_{\vec{q}}(P_{\vec{q}}^\dagger P_{\vec{q}} + \omega_{\mathrm{TO}}^2 Q_{\vec{q}}^\dagger Q_{\vec{q}})$ is the portion of the Hamiltonian that describes the long-wavelength TO phonons in the harmonic approximation,

$$H_{\mathrm{EM}} = \tfrac{1}{2}\textstyle\sum_{\vec{q}}[\Pi_{\vec{q}}^\dagger \Pi_{\vec{q}} + (c^2q^2/\epsilon_0)A_{\vec{q}}^\dagger A_{\vec{q}}]$$

is the Hamiltonian of the EM field in the absence of coupling to the lattice, and

$$H_{\mathrm{EM\text{-}ph}} = -\left(\frac{4\pi}{\epsilon_0 V_c m}\right)^{1/2} e^* \sum_{\vec{q}} P_{\vec{q}}^\dagger A_{\vec{q}} + \frac{2\pi e^{*2}}{\epsilon_0 V_c m}\sum_q A_{\vec{q}}^\dagger A_{\vec{q}}$$

describes the coupling between the TO mode and the EM field. In this expression, e^* is the dipole moment effective charge of the mode. The form given for each of the three terms just described may be derived from the Lagrangian introduced by Hopfield[6] that describes the interaction between classical polarization waves in crystals and the EM field. We consider only transverse modes in the present work.

Finally, Eq. (8) contains an anharmonic term $H_A(\{Q_{\vec{q}}\})$ that will cause the long-wavelength TO modes to acquire a finite lifetime. The notation is chosen to stress the fact that H_A depends only on the normal coordinates $Q_{\vec{q}}$ of the phonons, i.e., the momenta $P_{\vec{q}}$ do not enter H_A.

The Green's function $G_{AB}^R(t)$ introduced in Sec. II satisfies the equation of motion (with $\hbar = 1$)

$$i\frac{dG_{AB}^R}{dt} = \delta(t)\langle[A, B]\rangle + \langle\langle[A(t), H],\ B(0)\rangle\rangle , \quad (9)$$

where H is the Hamiltonian of Eq. (8). We let

$$D_{QQ}(\vec{q}, \omega) = \int \frac{dt}{2\pi}\,\langle\langle Q_{\vec{q}}^\dagger(t),\ Q_{\vec{q}}(0)\rangle\rangle\, e^{i\omega t} , \quad (10a)$$

$$P_{\pi Q}(\vec{q}, \omega) = \int \frac{dt}{2\pi}\,\langle\langle \Pi_{\vec{q}}^\dagger(t),\ Q_{\vec{q}}(0)\rangle\rangle\, e^{i\omega t} , \quad (10b)$$

$$P_{Q\pi}(\vec{q}, \omega) = \int \frac{dt}{2\pi}\,\langle\langle Q_{\vec{q}}^\dagger(t),\ \Pi_{\vec{q}}(0)\rangle\rangle\, e^{i\omega t} , \quad (10c)$$

and $G_{\pi\pi}(\vec{q}, \omega) = \int \frac{dt}{2\pi}\,\langle\langle \Pi_{\vec{q}}^\dagger(t),\ \Pi_{\vec{q}}(0)\rangle\rangle\, e^{i\omega t}$. (10d)

The spectral densities that appear in Eq. (7) may

be constructed from these functions by the procedure outlined in Sec. II.

Upon employing Eqs. (9) and (10), one finds

$$(\omega_{TO}^2 - \omega^2) D_{QQ}(\vec{q}, \omega) + \Omega_p P_{\pi Q}(\vec{q}, \omega) - \mathcal{G}_{PQ}(\vec{q}, \omega) = -1/2\pi \ , \tag{11}$$

where $\Omega_p^2 = 4\pi e^{*2}/mV_c\epsilon_0$, and we have introduced

$$\mathcal{G}_{PQ}(\vec{q}, \omega) = \int \frac{dt}{2\pi} \langle\langle [P_{\vec{q}}^{\dagger}(t), H_A], Q_{\vec{q}}(0)\rangle\rangle e^{i\omega t} \ .$$

The effect of the damping of the lattice motion makes its appearance through the term $\mathcal{G}_{PQ}(\vec{q}, \omega)$.

The function $\mathcal{G}_{PQ}(\vec{q}, \omega)$ may be written in the form

$$\mathcal{G}_{PQ}(\vec{q}, \omega) = 2\omega_{TO}\, \Pi(\vec{q}, \omega) D_{QQ}(\vec{q}, \omega) \ , \tag{12a}$$

where $\Pi(\vec{q}, \omega)$ is the phonon proper self-energy.

We shall make one important assumption. Consider the lowest-order contribution to Π from the presence of third-order anharmonicity. The diagram associated with this contribution is given in Fig. 3. The wave vector $\vec{q}$ that will concern us here is very small, when compared to the distance of the Brillouin-zone boundary from the origin of $\vec{k}$ space. When one computes the contribution to Π from a diagram like that in Fig. 3, phase-space considerations show that the dominant contribution comes from large values of $\vec{k}$, where the joint density of states is large. These short-wavelength modes are not affected by the coupling of the lattice to the transverse EM field. The polariton effects are confined to a small volume of phase space near the origin. Thus, to an excellent approximation, we may presume the proper self-energy of Eq. (12a) is unaffected by the interactions responsible for the polariton character of the long-wavelength TO modes, i.e., we suppose $\Pi(\vec{q}, \omega)$ is unaffected by the presence of the term $H_{\text{EM-ph}}$ in Eq. (8). Indeed, for our purposes, one may replace $\Pi(\vec{q}, \omega)$ by $\Pi(\vec{0}, \omega)$ to a very good approximation. We shall do this in the discussion below.

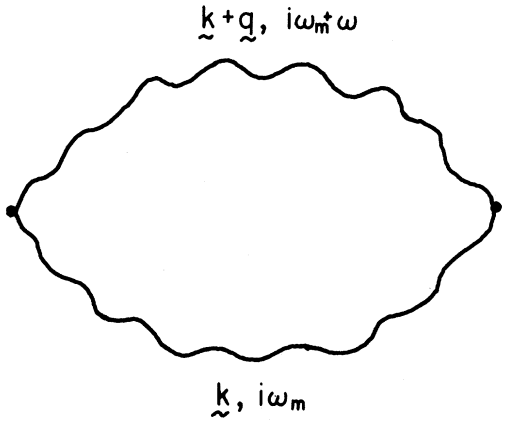

FIG. 3. First term in the phonon proper self-energy, in the presence of cubic anharmonicity.

With these comments in mind, Eq. (11) may be written

$$[\omega_{TO}^2 - 2\omega_{TO}\Pi(\omega) - \omega^2] D_{QQ}(\vec{q}, \omega) + \Omega_p P_{\pi Q}(\vec{q}, \omega) = -1/2\pi \ . \tag{12b}$$

In a similar fashion, the equation of motion for $P_{\pi Q}(\vec{q}, \omega)$ may be obtained. We find

$$(c^2q^2/\epsilon_0 + \Omega_p^2 - \omega^2) P_{\pi Q}(\vec{q}, \omega) - \Omega_p[\omega_{TO}^2 - 2\omega_{TO}\Pi(\omega)] \times D_{QQ}(\vec{q}, \omega) = +\Omega_p/2\pi \ . \tag{13}$$

Equations (12b) and (13) are two algebraic equations that may be solved for $P_{\pi Q}(\vec{q}, \omega)$ and $D_{QQ}(\vec{q}, \omega)$:

$$D_{QQ}(\vec{q}, \omega) = \frac{1}{2\pi} \times \frac{\omega^2 - c^2q^2/\epsilon_0}{[\omega^2 - \omega_{TO}^2 + 2\omega_{TO}\Pi(\omega)]\,[\omega^2 - (c^2q^2/\epsilon_0)] - \Omega_p^2\omega^2} \tag{14}$$

and $$P_{\pi Q}(\vec{q}, \omega) = -\Omega_p\omega^2[\omega^2 - c^2q^2/\epsilon_0]^{-1} D_{QQ}(\vec{q}, \omega) \ . \tag{15}$$

By proceeding in a similar way, one may obtain two coupled equations for the quantities $P_{Q\pi}(\vec{q}, \omega)$ and $G_{\pi\pi}(\vec{q}, \omega)$. We find

$$P_{Q\pi}(\vec{q}, \omega) = P_{\pi Q}(\vec{q}, \omega) \tag{16}$$

and

$$G_{\pi\pi}(\vec{q}, \omega) = \frac{1}{2\pi} \times \frac{[\omega^2 - \omega_{TO}^2 + 2\omega_{TO}\Pi(\omega)]c^2q^2/\epsilon_0 + \Omega_p^2\omega^2}{[\omega^2 - \omega_{TO}^2 + 2\omega_{TO}\Pi(\omega)]\,[\omega^2 - c^2q^2/\epsilon_0] - \Omega_p^2\omega^2} \ , \tag{17a}$$

$$G_{\pi\pi}(\vec{q}, \omega) \equiv \frac{1}{2\pi} \frac{c^2q^2/\epsilon_0}{\omega^2 - c^2q^2/\epsilon_0} + \frac{\Omega_p^2\omega^4}{(\omega^2 - c^2q^2/\epsilon_0)^2} D_{QQ}(\vec{q}, \omega) \ . \tag{17b}$$

The form of $G_{\pi\pi}$ exhibited in Eq. (17b) will be convenient for our purposes. Note from Eq. (17a) that this function has no pole at the free-photon frequency $\omega = cq/\sqrt{\epsilon_0}$.

There is one point in the derivation of Eqs. (16) and (17) that we mention. Upon writing the equations of motion for $P_{Q\pi}$ and $G_{\pi\pi}$, one encounters the function

$$\mathcal{G}_{P\pi}(\vec{q}, \omega) = \frac{1}{i} \int \frac{dt}{2\pi} e^{i\omega t} \langle\langle [P_{\vec{q}}^{\dagger}(t), H_A], \Pi_{\vec{q}}(0)\rangle\rangle \ .$$

Upon examining the structure of the diagrams that contribute to $\mathcal{G}_{P\pi}$, one may show that

$$\mathcal{G}_{P\pi}(\vec{q},\omega)=\Pi(\omega)P_{Q\pi}(\vec{q},\omega)\ ,$$

where $\Pi(\omega)$ is the proper self-energy of the phonon introduced earlier.

Upon inserting the results of Eqs. (14)–(17) into Eq. (7), the Raman efficiency may be written in the form

$$\frac{d^2S}{d\Omega\,d\omega}=\frac{\hbar V_c\omega_I^4}{mc^4}\left|\sum_{\alpha\beta\gamma}\hat{e}_\alpha(I)\hat{e}_\beta(S)\hat{\epsilon}_\gamma^{(\mathrm{ph})}\epsilon_{\alpha\beta\gamma}\right|^2[1+n(\omega)]\times\left(a+b\,\frac{4\pi e^*}{V_c}\,\frac{\omega^2}{c^2q^2-\epsilon_0\omega^2}\right)^2\alpha_{QQ}(\vec{q},\omega). \tag{18}$$

To compute $\alpha_{QQ}(\vec{q},\omega)$, we need to note that

$$\Pi(\omega\pm i\epsilon)=\Delta(\omega)\mp i\Gamma(\omega)\ , \tag{19}$$

where $\Delta(\omega)$ is the real part of the self-energy, and $\Gamma(\omega)$ is the imaginary part. For the discussion below, one should recall that $\Gamma(\omega)$ and $\Delta(\omega)$ form a Kramers-Krönig transform pair. Let us define the quantity

$$\tilde{\omega}_{\mathrm{TO}}=\omega_{\mathrm{TO}}-2\omega_{\mathrm{TO}}\Delta(\omega)\ . \tag{20}$$

If we replace ω by ω_{TO} on the right-hand side of this expression, $\tilde{\omega}_{\mathrm{TO}}$ is then the renormalized TO phonon frequency, corrected for the frequency shifts introduced by the presence of anharmonicity. While we shall not indicate explicitly that $\tilde{\omega}_{\mathrm{TO}}$ is frequency dependent, one should keep in mind that this quantity does depend on the frequency transfer ω through its dependence on $\Delta(\omega)$.

From Eq. (14), and the definition of $\alpha_{QQ}(\vec{q},\omega)$ given above, we find

$$\alpha_{QQ}(\vec{q},\omega)=\frac{2}{\pi}\times\frac{\omega_{\mathrm{TO}}\Gamma(\omega^2-c^2q^2/\epsilon_0)^2}{[\omega^2-\omega_-^2(\vec{q})]^2[\omega^2-\omega_+^2(\vec{q})]^2+4\omega_{\mathrm{TO}}^2\Gamma^2(\omega^2-c^2q^2/\epsilon_0)^2}\ . \tag{21}$$

In this expression, Γ is the imaginary part of the proper self-energy, and $\omega_\pm(\vec{q})$ are the frequencies of the polariton modes in the absence of damping, i.e.,

$$\omega_\pm^2(\vec{q})=\tfrac{1}{2}\{c^2q^2/\epsilon_0+\Omega_p^2+\tilde{\omega}_{\mathrm{TO}}^2\}\pm\tfrac{1}{2}\{(c^2q^2/\epsilon_0+\Omega_p^2+\tilde{\omega}_{\mathrm{TO}}^2)^2-(4c^2q^2/\epsilon_0)\tilde{\omega}_{\mathrm{TO}}^2\}^{1/2}\ . \tag{22}$$

Thus, one finds for the Raman efficiency the result

$$\frac{d^2S}{d\Omega\,d\omega}=\frac{\hbar V_c\omega_I^4}{\pi mc^4}\left|\sum_{\alpha\beta\gamma}\hat{e}_\alpha(I)\hat{e}_\beta(S)\hat{e}_\gamma^{(\mathrm{ph})}\epsilon_{\alpha\beta\gamma}\right|^2\times[1+n(\omega)]\left[a+b\left(\frac{4\pi e^*}{V_c}\right)\frac{\omega^2}{c^2q^2-\epsilon_0\omega^2}\right]^2\times\frac{\omega_{\mathrm{TO}}\Gamma(\omega^2-c^2q^2/\epsilon_0)^2}{[\omega^2-\omega_-^2(\vec{q})]^2[\omega^2-\omega_+^2(\vec{q})]^2+4\omega_{\mathrm{TO}}^2\Gamma^2(\omega^2-c^2q^2/\epsilon_0)^2}\ . \tag{23}$$

In this expression, recall that $\omega=\omega_I-\omega_S$ is the frequency shift of the photon, and $\vec{q}=\vec{k}_I-\vec{k}_S$ is the change in wave vector of the incident photon.

Our result in Eq. (23) reduces to the standard expression for the Raman cross section in the limit as $\Gamma\to 0$. When $\Gamma\to 0$, the spectral density α_{QQ} becomes

$$\lim_{\Gamma\to 0}\alpha_{QQ}(\vec{q},\omega)=\frac{1}{2\tilde{\omega}_{\mathrm{TO}}}S_{\mathrm{ph}}(\omega)\times[\delta(\omega-\omega_-(\vec{q}))-\delta(\omega+\omega_-(\vec{q}))+\delta(\omega-\omega_+(\vec{q}))-\delta[\omega+\omega_+(\vec{q})]\ ,$$

where $S_{\mathrm{ph}}(\omega)$ is the phonon strength function introduced in earlier discussions.[7]

In the limit as $\Gamma\to 0$, scatterings that involve polaritons on the upper branch fail to conserve wave vector and energy. Thus, we may drop the terms containing $\omega_+(\vec{q})$. Then

$$\lim_{\Gamma\to 0}\frac{d^2S}{d\Omega\,d\omega}=\frac{\hbar V_c\omega_I^4}{2mc^4\tilde{\omega}_{\mathrm{TO}}}\left|\sum_{\alpha\beta\gamma}\hat{e}_\alpha(I)\hat{e}_\beta(S)\hat{\epsilon}_\gamma^{(\mathrm{ph})}\epsilon_{\alpha\beta\gamma}\right|^2\times[1+n(\omega)]\left[a+b\left(\frac{4\pi e^*}{V_c}\right)\frac{\omega^2}{c^2q^2-\epsilon_0\omega^2}\right]^2\times S_{\mathrm{ph}}(\omega)[\delta(\omega-\omega_-(\vec{q}))-\delta(\omega+\omega_+(\vec{q}))]\ . \tag{24}$$

This is the result employed in earlier work, which ignored the effect of the damping of the lattice motion.[8]

For the case where damping of the lattice motion is present, Eq. (23) may be employed to give a description of the Raman line for all scattering angles, from the small angle (polariton) regime to the large angle region. When the scattering angle is large, say, near 90°, then

$$cq/\sqrt{\epsilon_0}\gg\omega\ .$$

In this limit, $\omega_-(\vec{q})\approx\tilde{\omega}_{\mathrm{TO}}$, and $\omega_+(\vec{q})\approx cq/\sqrt{\epsilon_0}$. Equation (23) reduces to

$$\frac{d^2S}{d\Omega\,d\omega}=\frac{\hbar V_c\omega_I^4}{\pi mc^4}\left|\sum_{\alpha\beta\gamma}\hat{e}_\gamma(I)\hat{e}_\beta(S)\hat{\epsilon}_\gamma^{(\mathrm{ph})}\epsilon_{\alpha\beta\gamma}\right|^2\times[1+n(\omega)]a^2\,\frac{2\omega_{\mathrm{TO}}\Gamma}{[\omega^2-\tilde{\omega}_{\mathrm{TO}}^2]^2+4\omega_{\mathrm{TO}}^2\Gamma^2}\ . \tag{25}$$

One thus has a roughly Lorentzian line (for small Γ) centered about the frequency $\tilde{\omega}_{\mathrm{TO}}$. This is the result to be expected for large scattering angles, outside the polariton regime.

In his study of the Raman spectra of GaP in the region of large wave-vector transfer, Barker found a line shape for scattering produced by the TO mode that deviated strongly from the Lorentzian form. In his analysis of the data, he obtained information about the frequency dependence of $\Gamma(\omega)$ and $\Delta(\omega)$ in the neighborhood of the TO frequency $\tilde{\omega}_{TO}$. The study of the intrinsic width of the polariton in GaP by Raman scattering should allow the study of the frequency dependence of Δ and Γ over a wide frequency range. In effect, one can sweep the center of the line over a wide range of frequencies below $\tilde{\omega}_{TO}$. The study of the line shape as a function of scattering angle thus should yield information about the frequency dependence of the phonon proper self-energy over a region of frequency large compared to the intrinsic width of the TO mode.

IV. SOME DETAILED PROPERTIES OF POLARITON SPECTRA IN PRESENCE OF DAMPING OF LATTICE

In this section, we present the results of some detailed numerical studies of the shape and position of the polariton line, as a function of scattering angle. In all the calculations presented below, we have presumed that the imaginary part of the proper self-energy Γ is independent of frequency, and we have taken $\tilde{\omega}_{TO}$ to be equal to ω_{TO}. As discussed above, the experimental study of deviations in the spectra from the results obtained on this basis in principle contain useful quantitative information about the magnitude and frequency dependence of the phonon proper self-energy.

In the calculations, we have chosen parameters appropriate to ZnSe. The angular dependence of the Raman intensity in the polariton regime has been studied by Ushioda,[8] and the parameters appropriate to ZnSe are presented in the thesis cited in Ref. 8. One has $\omega_{TO} = 207\ \mathrm{cm}^{-1}$, $\omega_{LO} = 253\ \mathrm{cm}^{-1}$, and $\epsilon_0 = 5.75$. Also, for this crystal, analysis of the angular dependence of the scattering intensity in the polariton regime gives

$$\gamma = (b/a)(4\pi e^*/\epsilon_0 V_c) \simeq -2.5 \ .$$

To proceed further, we need to relate the wave-vector transfer q to the scattering angle θ between the direction of the incoming and outgoing radiation, and the frequency transfer $\omega = \omega_I - \omega_S$. If n_I and n_S are the indices of refraction of the incident and scattered light, then

$$c^2q^2 = c^2\left|\vec{k}_I - \vec{k}_S\right|^2 = n_I^2\omega_I^2 + n_S^2\omega_S^2 - 2n_Sn_I\omega_S\omega_I\cos\theta \ . \tag{26}$$

Since the frequency transfer ω is small compared to ω_I for incident frequencies in the visible, one has

$$n_S = n_I - \omega\left(\frac{\partial n}{\partial \omega}\right)_{\omega_I} \ .$$

For small θ, and small ω, Eq. (26) may then be written

$$c^2q^2 = n_I^2\omega_I^2\theta^2 + \left[n_I + \omega_I\left(\frac{\partial n}{\partial \omega}\right)_{\omega_I}\right]^2\omega^2 \ . \tag{27}$$

Equation (27) gives the relation between θ and q, for a given frequency transfer. In the absence of damping, the polariton frequency observed at a particular θ may be obtained graphically by superimposing the relation between ω and q provided by Eq. (27) on a plot of the polariton dispersion relation. This procedure is illustrated in Fig. 1(a). The dotted lines have been obtained from Eq. (27). The index of refraction n_I of ZnSe at the 6328-Å He-Ne line is 2.58,[8] and $(\partial n/\partial\omega)\omega_I = 2.49 \times 10^{-5}/\mathrm{cm}^{-1}$.[9] These are the numbers we shall employ in the calculations described below.

In Fig. 4 we present a plot of the angular dependence of the peak scattering intensity in the polariton regime. The curves have been computed for the case where $\Gamma = 2.5\ \mathrm{cm}^{-1}$. The solid line is computed for the value of γ appropriate to ZnSe, i.e.,

$$\gamma = -2.5 \equiv \gamma_- \ .$$

To illustrate the effect of the sign of γ on the angular dependence of the scattering intensity, the dotted curve in Fig. 4 is a plot of the angular dependence of the scattering intensity for the case

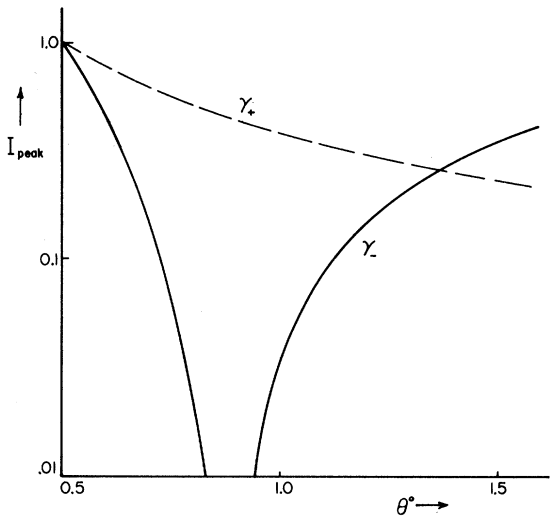

FIG. 4. Dependence of the peak intensity of the Raman line on scattering angle, for parameters appropriate to ZnSe. See the text for a definition of the quantities γ_+ and γ_-. Both curves are arbitrarily normalized to unity at 0.5°.

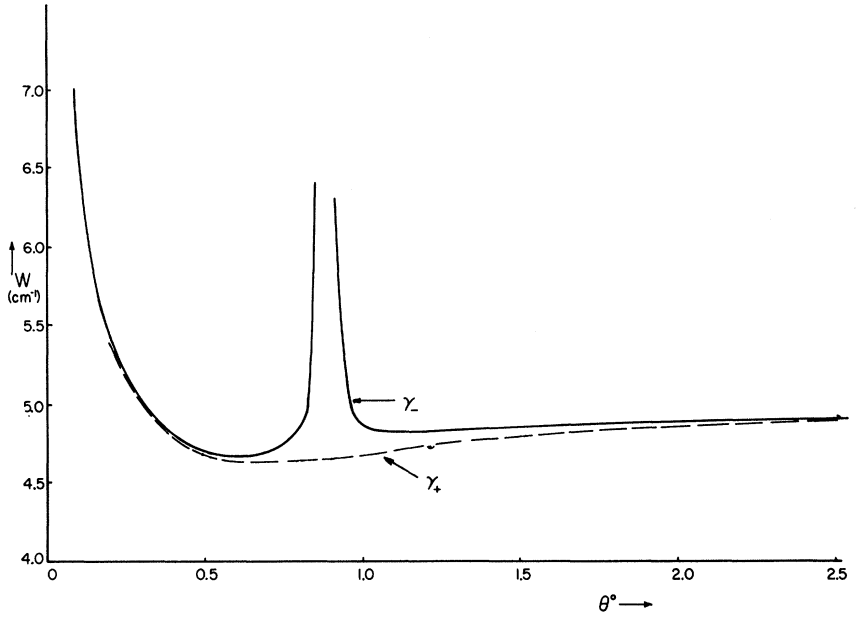

FIG. 5. Intrinsic full width W at half-maximum of the Raman line in ZnSe, calculated for $\Gamma = 2.5$ cm^{-1} (the large-angle TO phonon line then has a width of 5 cm^{-1}). At $\theta = 0$, both curves approach a finite value.

where the sign of γ is reversed, i.e.,

$$\gamma = +2.5 \equiv \gamma_+ \ .$$

The minimum in the scattering intensity that appears in the solid curve occurs because when γ is negative, the electro-optic and atomic displacement contributions to the cross section interfere destructively in the polariton regime. A comparison between the data on ZnSe and the predictions of the polariton theory has been given earlier by Ushioda.[8] We present the curves of Fig. 4 to provide a reference for our later discussion.

In Fig. 5, the dependence of the full width of the Raman line at half-maximum on scattering angle is given. The width plotted in this figure is the intrinsic width of the line. This is the width one would observe if the incident beam is perfectly collimated and the detector were to subtend an infinitesimal solid angle. These curves are computed for the case where $\Gamma = 2.5$ cm^{-1}, and γ assumes the two values employed in Fig. 4.

There are two prominent features evident in the curves of Fig. 5. The linewidth increases rapidly as $\theta \to 0$, to a finite value at $\theta = 0$. Also, when $\gamma < 0$, the linewidth becomes very large (in fact, infinite) at the angle corresponding to the mini-

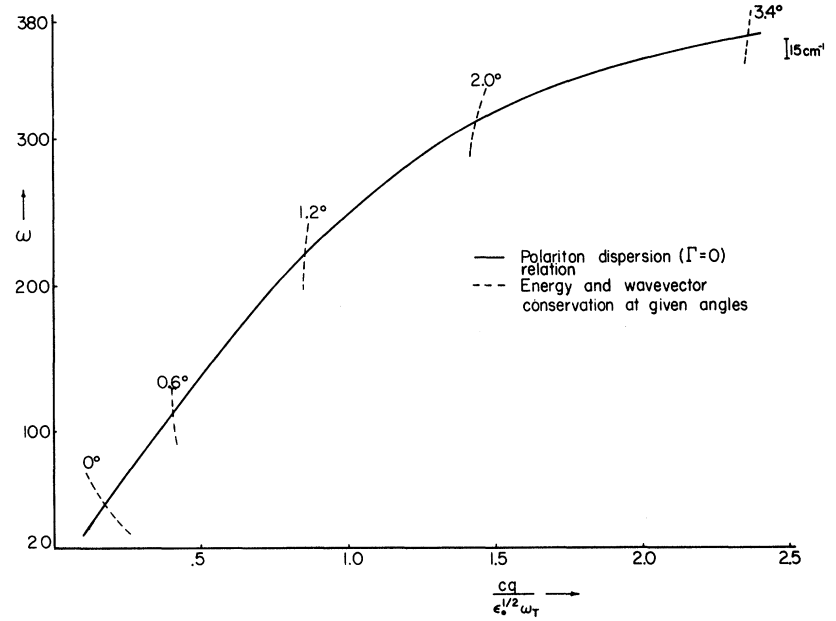

FIG. 6. Lower branch of the polariton dispersion curve for ZnO, with the relation between frequency and wave-vector transfer for various scattering angles also included.

mum in the scattering intensity. The first of these features comes about because for very small θ, the curve of ω versus q obtained from Eq. (27) becomes nearly parallel to the undamped polariton curve (see Fig. 1). When this is so, and the damping of the lattice is introduced into the theory, the width in frequency of the line observed at fixed θ can become quite large as $\theta \to 0$. This happens even though the reduction in the phonon content of the lower branch of the polariton dispersion relation causes the width of the feature in the spectral density $G_{QQ}(\vec{q}, \omega)$ (considered as a function of ω for fixed q) to decrease markedly for small q, compared to the width at large wave vectors. For negative γ, Fig. 5 shows that the linewidth becomes very large near the minimum in the scattering intensity. This increase in linewidth comes about because at this scattering angle the factor multiplying G_{QQ} in Eq. (23) has a zero at the line center, and increases like ω^2 as one moves to the high or low frequency side of the line center. Thus, when θ assumes this special value, the scattered light is distributed over a range of frequency that is very broad compared to the intrinsic width of the TO mode.

We should like to illustrate the dependence of the intrinsic linewidth at very small angles on the kinematics of the scattering process by a second illustration. We have seen that for the case of ZnSe, the linewidth at small angles increases, because of the near tangency of the polariton dispersion curves, and the trajectories in the ω-q plane found from Eq. (27). The case of ZnO, for the geometry employed by Porto and his co-workers[10] in their study of polaritons in this material, offers an example of contrasting behavior. In their experiment, the incident photon is an ordinary wave and the scattered photon is an extraordinary wave. In Fig. 6, we plot the dispersion relation of the lower polariton branch of ZnO, and we have superimposed on this plot the relation between ω and q for various angles by using the kinematic condition analogous to Eq. (27). [See Eq. (2b) of the paper by Porto *et al.*[10]] Note that for small θ, the dashed curves cut across the polariton dispersion curve sharply, in contrast to the case of ZnSe. In Fig. 7, we plot the intrinsic Raman linewidth as a function of scattering angle for this case. One sees that the sharp upturn at small scattering angles that is such a prominent feature of Fig. 5 is not present in this case. For ZnO, the ratio γ is positive,[8] so no minimum in the angular dependence of the scattering efficiency is present.

Porto *et al.*[10] have reported that the width of the observed polariton line in ZnO increases as θ is decreased. These authors attribute this to the

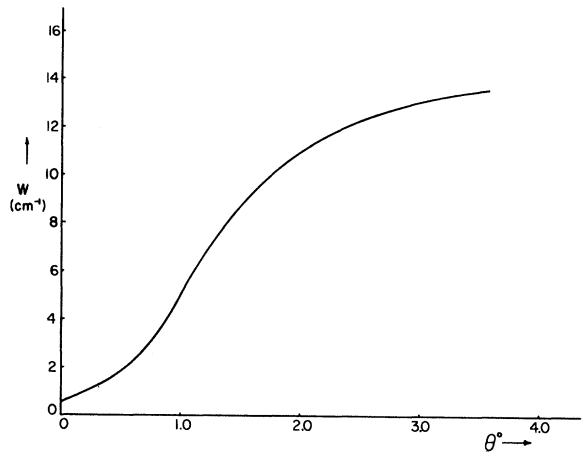

FIG. 7. Dependence of the intrinsic contribution to the full width of the Raman line at half-maximum, for the case of ZnO.

fact that their detector subtends a finite solid angle, and the laser beam is focused on the crystal. These features of the experimental apparatus will cause a broadening of the observed Raman line at small angles, where the polariton frequency depends strongly on wave vector. The results of the calculations described in the preceding paragraph support this contention, since we have seen that in ZnO, the kinematics of the scattering process cause the intrinsic width of the Raman line to decrease at small angles.

In general, we find that the Raman line is asymmetric in the polariton regime. The asymmetry arises because as the frequency transfer ω is varied for a fixed value of the scattering angle θ, the relative importance of the atomic displacement and electro-optic contributions to the scattering intensity also varies. Thus, the asymmetry becomes especially pronounced for $\gamma < 0$ in the vicinity of the minimum in the scattering intensity. In Fig. 8, we plot the asymmetry of the line as a function of scattering angle for the two cases $\gamma = \gamma_+ = 2.5$ and $\gamma = \gamma_- = -2.5$ and $\Gamma = 2.5\ \mathrm{cm}^{-1}$. The quantity A defined in the figure provides a measure of the asymmetry. When $\gamma > 0$, the line is found to be very nearly symmetric for all θ. When $\gamma < 0$, the large asymmetry near the minimum in the scattering intensity is evident. We know of no published experimental studies of the line shape of polariton spectra.

We conclude this section with a discussion of the angular dependence of the position of the center of the Raman line as a function of scattering angle. In Fig. 9, we present a graph that indicates the error introduced by the assumption that the polariton frequency and wave vector in the pres-

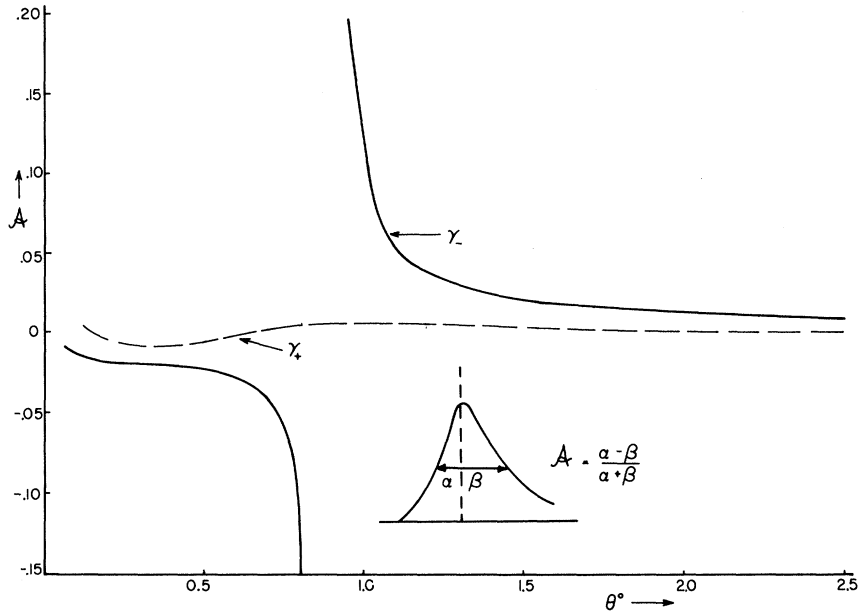

FIG. 8. Asymmetry parameter $\mathcal{A}$ as a function of scattering angle for ZnSe and the two values of γ described in the text. The quantity α refers to the low-frequency side of the Stokes line.

ence of damping may be computed by Eq. (1), after replacing $\epsilon(\omega)$ on the right-hand side by the real part $\epsilon_R(\omega)$ of the dielectric constant. The quantity Δ in Fig. 9 is the difference in frequency, the position of the peak we find from our calculations based on Eq. (18), and the peak position determined from the modified form of Eq. (1).

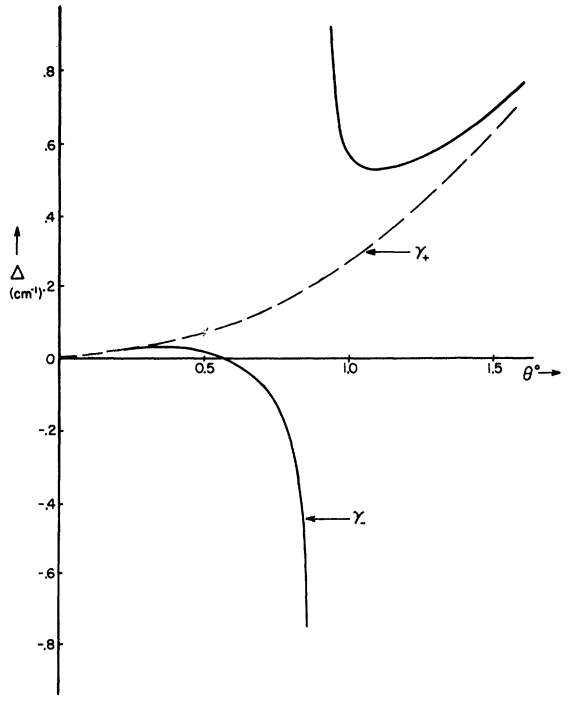

FIG. 9. Error Δ in the position of the center of the Raman line as a function of scattering angle for ZnSe when $\Gamma = 2.5$ cm^{-1}.

The curves are computed for both values of γ used previously and for $\Gamma = 2.5$ cm^{-1}. For both values of γ, one makes an appreciable error in using the modified form of Eq. (1) for angles greater than 1°, i.e., at this value of θ, the error in the peak position is the order of the linewidth. Note the anomaly in the position of the center of the line near the minimum in scattering intensity when γ is negative. In the region where the peak is shifted by a large amount the line is also very broad and asymmetric, and the scattering intensity near the peak is quite small. Our plot in Fig. 9 stops at $\theta = 1.5°$, because just slightly beyond this value of θ, the pseudodispersion curve computed from the modified Eq. (1) suffers its turnaround.

We have seen that from a physical point of view, the assumption that in the presence of damping one may interpret polariton spectra by employing the dispersion relation $c^2q^2/\omega^2 = \epsilon_R(\omega)$ is a procedure that cannot be justified. At the same time, we have noted that a number of practical difficulties occur when one tries to carry out the analysis by this means.

One must then inquire whether or not there exists a simple straightforward means of analyzing the angular dependence of the position of the peak of the polariton line, in order to relate these data to the properties of the crystal. In our numerical work, we have found in all cases studied that the simplest possible rule applies with remarkable accuracy, even when the lattice motion is rather heavily damped: The position of the peak as a function of scattering angle is very accurately fitted by using the polariton dispersion

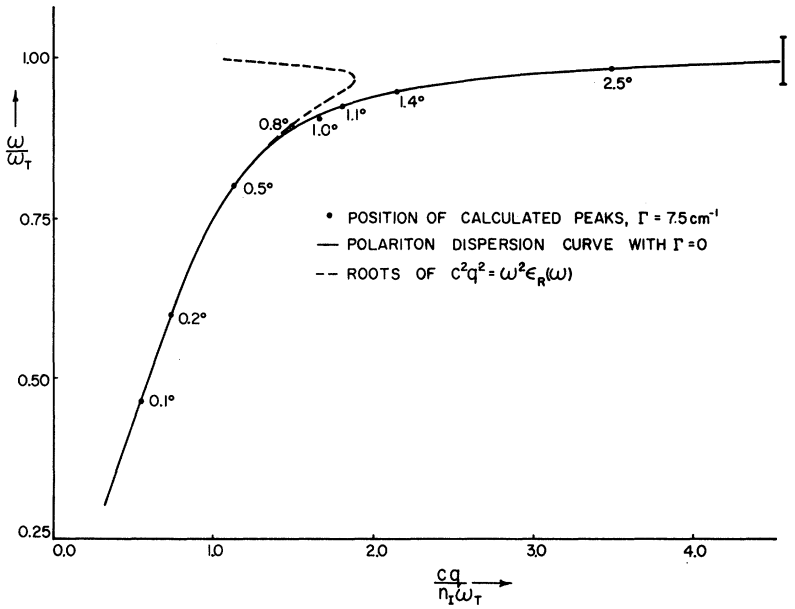

FIG. 10. Position of the center of the Raman line, as function of scattering vector as determined by the three methods discussed in the text. The quantity n_I is the refractive index at the incident light frequency. The vertical bar indicates the linewidth at large angles for the value of $\Gamma(7.5\ \mathrm{cm}^{-1})$ employed in this work. The remaining parameters have been chosen appropriate to ZnSe.

relation appropriate to the case where *no damping* at all is present, i.e., one uses the dispersion relation computed from Eq. (1), where the wave-vector transfer and scattering angle are related by Eq. (27). As an example of the kind of fit one obtains by this procedure, in Fig. 10 we present a plot of the polariton dispersion relation computed from Eq. (1) for parameters relevant to ZnSe (solid line). Superimposed on this plot we have the dispersion relation deduced by replacing $\epsilon(\omega)$ by $\epsilon_R(\omega)$ in Eq. (1) for the case where $\Gamma = 7.5\ \mathrm{cm}^{-1}$ (dotted line). For this value of Γ, the full width at half-maximum of the Raman line associated with the TO mode at large angles is 15 cm^{-1}. Thus, for this value of Γ, the mode is heavily damped. The dotted curve thus turns about at very small values of q, as one can see from the figure. Finally, on this graph we have placed a series of dots that give the relation between the peak frequency of the line and the wave-vector transfer for various values of θ. These points were determined by using Eq. (18) and the values of the parameters described above. To within graphical accuracy, the points fall directly on top of the solid line, except for a small and barely discernible anomaly in the vicinity of the minimum of the scattering intensity. We obtain similar results for the polaritons in ZnO. The results of our study indicate that even when the lattice motion is rather strongly damped, one should analyze the data employing Eq. (1), *without* modifying the right-hand side. We can present no physical reason why this simple rule is the correct one. We have found that it works very well for all of the cases we have examined.

ACKNOWLEDGMENTS

We have enjoyed many useful discussions of this work with A.A. Maradudin, E. Burstein, and S. Ushioda.

---

*Research supported in part by the Air Force Office of Scientific Research, Office of Aerospace Research, U.S. Air Force, under AFOSR Grant No. 68-1448.

†Alfred P. Sloan Foundation Fellow, 1968–1970.

[1]We shall simply cite a few examples of studies of polaritons which illustrate the kind of information one may obtain. See C. H. Henry and J. J. Hopfield, Phys. Rev. Letters 15, 964 (1965); S. Ushioda, Ph.D. thesis, University of Pennsylvania, 1969 (unpublished); A. Pinczuk, Ph. D. thesis, University of Pennsylvania, 1969 (unpublished); J. F. Scott, L. E. Cheesman, and S. P. S. Porto, Phys. Rev. 162, 834(1967); J. F. Scott, P. A. Fleury, and J. M. Worlock, *ibid.* 177, 1288(1969). A number of recent papers on the scattering of light by polaritons may be found in the *Proceedings of the International Conference on the Light Scattering Spectra of Solids, New York*, 1968, edited by G. B. Wright (Springer, New York, 1969).

[2]R. Loudon, Proc. Phys. Soc. (London) 82, 393 (1963).

[3]H. E. Puthoff, R. H. Pantell, B. G. Huth, and M. A. Chacon, J. Appl. Phys. 39, 2144 (1968). Also see paper *E*-1, in the *Proceedings of the International Conference on the Light Scattering Spectra of Solids, New York*, 1968, edited by G. B. Wright (Springer, New York, 1969).

[4]An interesting exception to this statement is pro-

vided by Barker's study of the TO phonon mode in GaP [A. S. Barker, Phys. Rev. 165, 917 (1968)]. The shape of the large-angle Raman line and IR absorption peak deviate strongly from the Lorentzian shape. Barker has carried out an analysis of his data by introducing a frequency-dependent damping factor. By studying the shape of the polariton spectrum of this mode, in principle one may extend Barker's analysis to a much wider range of frequencies. In essence, in the polariton regime, one can sweep the line center over a wide frequency region by varying the scattering angle.

[5]L. Van Hove, Phys. Rev. 95, 249 (1954); 95, 1374 (1954).

[6]J. J. Hopfield, Phys. Rev. 112, 1555 (1958).

[7]For example, see E. Burstein, S. Ushioda, A. Pinczuk, and J.F. Scott, 1969), paper A-1. in *Proceedings of the International Conference on Light Scattering Spectra of Solids, New York*, 1968, edited by G. B. Wright (Springer, New York, 1969).

[8]See the thesis of S. Ushioda cited in Ref. 1. Our expression for the scattering efficiency is one-half that given by Ushioda. We believe Ushioda's result is in error, because he presumed the cross section associated with both the Stokes and anti-Stokes line (in the classical theory) is proportional to the mean-square value $\langle u^2\rangle_T$ of the *total* relative displacement of the ions in the unit cell. In fact, $u(t)$ contains a positive frequency component u_+ and a negative frequency part u_-, with (in the classical theory) $\langle u_+^2\rangle_T = \langle u_-^2\rangle_T = \frac{1}{2}\langle u^2\rangle_T$. The cross section for anti-Stokes scattering is proportional to $\langle u_+^2\rangle_T$, while that for Stokes scattering is proportional to $\langle u_-^2\rangle_T$, rather than $\langle u^2\rangle_T$. Thus, Ushioda's cross section should be reduced by a factor of 2. This will bring it into agreement with our result.

[9]D. T. F. Marple, J. Appl. Phys. 35, 539 (1964).

[10]B. Tell, S. P. S. Porto, and T. C. Damen, Phys. Rev. Letters 16, 450 (1966).

PHYSICAL REVIEW B VOLUME 1, NUMBER 12 15 JUNE 1970

COMMENTS AND ADDENDA

The Comments and Addenda section is for short communications which are not of such urgency as to justify publication in Physical Review Letters and are not appropriate for regular Articles. It includes only the following types of communications: (1) comments on papers previously published in The Physical Review or Physical Review Letters; (2) addenda to papers previously published in The Physical Review or Physical Review Letters, in which the additional information can be presented without the need for writing a complete article. Manuscripts intended for this section may be accompanied by a brief abstract for information-retrieval purposes. Accepted manuscripts will follow the same publication schedule as articles in this journal, and galleys will be sent to authors.

Cooling Curve in a One-Dimensional Crystal

K. J. Mork
University of Trondheim, Norges Laererhøgskole, Trondheim, Norway
(Received 19 January 1970)

A region of $2N+1$ particles in a harmonic one-dimensional crystal is given temperature T_0 at time $t=0$. The central particle in this region cools down as follows[1]:

$$T(t) = T_0 \sum_{n=-N}^{N} J_n^2(Nt) , \qquad (1)$$

where t is a suitable dimensionless time variable. By very complicated asymptotics Rubin[1] was able to determine the following limiting behavior:

$$\lim_{N\to\infty} T(t)/T_0 = 1, \qquad \text{for } t<1$$

$$= 2\pi^{-1}\arcsin(1/t), \quad \text{for } t>1 . \qquad (2)$$

The present note demonstrates how this limiting cooling curve may be found in a simple manner. The standard representation[2]

$$J_n^2(z) = 2\pi^{-1}\int_0^{\pi/2} J_0(2z\sin\phi)\cos 2n\phi\, d\phi$$

allows the summation over n in Eq. (1) to be performed. Introducing a new variable $x = 2N\sin\phi$, we obtain

$$T(t)/T_0 = 2\pi^{-1}\int_0^{2N} dx\, x^{-1} J_0(xt) \times \sin[2N\arcsin(x/2N)] + J_N^2(Nt) . \qquad (3)$$